Order in Microcontact Printed Self-Assembled Monolayers

N. B. Larsen,[‡,§] H. Biebuyck,* E. Delamarche,[†] and B. Michel[†]

Contribution from the IBM Research Division, Zurich Research Laboratory,
8803 Rüschlikon, Switzerland, and CISMI, University of Copenhagen, Denmark

Abstract: Self-assembled monolayers (SAMs) on Au(111) formed by microcontact printing of dodecanethiol and investigated by scanning tunneling microscopy and wettability measurements have, under certain conditions, characteristics indistinguishable from SAMs formed from solutions of dodecanethiol in ethanol. The monolayer product of microcontact printing demonstrates a sensitivity to the concentration of thiol used to ink a poly-(dimethylsiloxane) (PDMS) stamp needed to make the print and an insensitivity to its duration of contact, for times >0.3 s, with the gold substrate. The wettability of the SAM, the distribution of domains within the monolayer, their size and organizational state, and the pattern of depressions on the surface each are reproducibly controlled by simply changing the concentration of dodecanethiol applied to the stamp. The inferred mode of growth of printed SAMs shares many features of monolayer formation through the gas phase of a thiol and corresponds to a highly controlled and self-limiting delivery of thiol from the interior parts of the PDMS. Our study shows that printed SAMs provide a wonderful opportunity to change controllably the order in monolayers at the nanometer scale and to examine its effects on microscopic and macroscopic properties of these films.

1. Introduction

This paper examines the type and degree of microscopic order present in self-assembled monolayers (SAMs) formed by microcontact printing. Microcontact printing (μCP) is a relatively new approach to the formation of SAMs that uses conformal contact between an elastomeric stamp and a substrate to deliver molecules "inked" on the surface of the stamp to the substrate. The technique can form monolayers of alkanethiols on gold[1,2] and alkylsilanes on hydroxylated surfaces.[3,4] Its ability to transfer SAMs in patterns with sub-100 nm resolution onto planar and nonplanar[5] substrates makes this approach appealing for research, and possibly technological, purposes. SAMs patterned by μCP allow facile and differential control over many properties of an interface including its wettability,[6,7] its susceptibility to nucleation,[8,9] and its barrier to chemical access of the underlying substrate.[1]

We wanted to answer two questions associated with the characteristics of alkanethiol monolayers printed on gold by μCP. First, are printed SAMs structurally equivalent to those formed in solution? We chose scanning tunneling microscopy (STM) as our probe of the molecular arrangement in the monolayer, because it investigates order in SAMs in real space with sub-Ångstrøm resolution.[10] This capability was particularly relevant to us because we expected defects in the organization of the monolayer at the nanometer scale to dominate the chemical properties of the interface. Aberrant etching processes that interfere with the quality of high-contrast pattern transfer in fabrication, for example, may occur after disruption of just a few molecules in a SAM.[11] We used dodecanethiol (DDT) as our monolayer forming material. DDT forms ordered SAMs on gold having a thickness of ≈1.3 nm and exposing a surface of low free energy (≈20 mJ/m^2). Most of the properties of DDT monolayers resemble those of SAMs of hexadecanethiol that provide the best resistance to a cyanide/oxygen etchant,[12,13] whereas the smaller thickness of DDT monolayers allows STM studies at practically attainable tunneling currents (1−10 pA). SAMs of DDT have been extensively characterized providing a well-founded basis for structural comparisons. Most of the demonstrations of μCP to date used polycrystalline gold films. The topography of this gold prevents STM observation of individual molecules in SAMs, however, because its features convolute with those of the monolayer. Instead, we printed DDT onto epitaxial Au(111) films evaporated on mica that allowed facile differentiation of gold and monolayer. We expected to draw useful inferences about the processes of μCP by investigating this system.

The second question posed in our study was how the initial application of the alkanethiol solution to the surface of the stamp (termed "inking") affected the order in printed SAMs. In the limit of no alkanethiol in the inking solution, a SAM can obviously not form. We wanted to know what thiol concentration was necessary to make high-quality monolayers and how the inking solutions affected the structure of the film when its

---

* To whom correspondence should be addressed. e-mail: hbi@zurich.ibm.com.

[†] IBM Research Division, Zurich Research Laboratory.

[‡] CISMI.

[§] Current address: Risoe National Laboratory, DK-4000 Roskilde, Denmark.

[⊗] Abstract published in *Advance ACS Abstracts,* March 1, 1997.

(1) Kumar, A.; Whitesides, G. M. *Appl. Phys. Lett.* **1993**, *63*, 2002−2004.

(2) Kumar, A.; Biebuyck, H. A.; Whitesides, G. M. *Langmuir* **1994**, *10*, 1498−1511.

(3) Xia, Y.; Mrksich, M.; Kim, E.; Whitesides, G. M. *J. Am. Chem. Soc.* **1995**, *117*, 9576−9577.

(4) St. John, P. M.; Craighead, H. G. *Appl. Phys. Lett.* **1996**, *68*, 1022−1024.

(5) Jackman, R. J.; Wilbur, J. L.; Whitesides, G. M. *Science* **1995**, *269*, 664−666.

(6) Kumar, A.; Whitesides, G. M. *Science* **1994**, *263*, 60−62.

(7) Biebuyck, H. A.; Whitesides, G. M. *Langmuir* **1994**, *10*, 2790−2793.

(8) Jeon, N. L.; Nuzzo, R. G.; Xia, Y.; Mrksich, M.; Whitesides, G. M. *Langmuir* **1995**, *11*, 3024−3026.

(9) Gorman, C. B.; Biebuyck, H. A.; Whitesides, G. M. *Chem. Mater.* **1995**, *7*, 252−254.

(10) Delamarche, E.; Michel, B.; Biebuyck, H. A.; Gerber, Ch. *Adv. Mater.* **1996**, *8*, 719−729.

(11) Biebuyck, H.; Larsen, N. B.; Delamarche, E.; Michel, B. *IBM J. Res. Develop.* **1997**, *41*, (in press).

(12) Zhao, X. -M.; Wilbur, J. L.; Whitesides, G. M. *Langmuir* **1996**, *12*, 3257−3264.

(13) Chailapakul, O.; Sun, L.; Xu, C.; Crooks, R. M. *J. Am. Chem. Soc.* **1993**, *115*, 12459.

concentration was less than optimal. Microcontact printing is principally a "dry" process: ideally, no liquid drops are present on the surface of the stamp as it makes contact with the substrate. Typically, inking of a stamp occurs by brushing its surface with a cotton swab dipped in a millimolar solution of an alkanethiol in ethanol. Visual inspection indicates that the majority of the solvent, present on the surface in the form of small (<50 μm radii) drops, evaporates within seconds leaving an outwardly dry stamp and presumably concentrating the less volatile alkanethiol in its surface region. Transient contact (seconds) between the inked stamp and a gold surface leaves behind a SAM. This process of inking makes the actual concentration of thiol in the surface region of the stamp difficult to determine, particularly because there is migration of some undetermined fraction of the thiol into the elastomer, usually made from poly(dimethylsiloxane) (PDMS).

In an early part of our study we had several indications (varying wettability of the sample, characteristics of the etching barrier, and the degree and type of nanometer-scale order in SAMs of DDT) that using a swab to apply the ink gave unpredictable results in conjunction with dilute (<10 mM) solutions of DDT in ethanol. We therefore investigated another inking technique: A drop of freshly prepared (<1 h) solutions of DDT in ethanol was applied to the surface of the stamp. Equilibration between the surface of the stamp and the drop proceeded for 30 s; the drop was laterally ejected from the surface under a stream of N_2, which was maintained for another 30 s. Although this procedure still did not establish the absolute concentration of thiol on the surface of the stamp, we expected it to provide a well-defined starting point for a relative comparison of the effects of ink concentration on μCP. When followed rigorously, our method of inking stamps gave excellent reproducibility of such properties of the printed SAMs as their wettability and microscopic order and provided deterministic and facile control over these parameters by changes in the concentration of DDT.

Briefly, our study showed that SAMs of DDT formed by μCP have an achievable order indistinguishable from those formed in solution. Inking the stamp as above with >10 mM of DDT in ethanol gave SAMs on gold having the same organization and distribution of defects and depressions as those SAMs prepared by equilibration of gold in solution. Lowering the concentration of DDT inked on the stamp to <10 mM provided a significant deviation in the degree and type of order observed in the resulting SAMs. Wettability studies of printed SAMs by water and hexadecane corroborated the findings from STM. Printing with solutions more concentrated than 10 mM resulted in contact angles and hysteresis measures indistinguishable from those found for monolayers formed in solution. Reducing the alkanethiol concentration in the solution inked on the stamp gave lower contact angles and higher hysteresis in the wettability that strongly correlated with the concentration of thiol. These changes were consistent with a general evolution in the structure of the monolayer. Generally, STM showed that domains exhibiting the well-known ($\sqrt{3} \times \sqrt{3})R30°$ structure increased in size in the printed SAMs as the concentration of thiol in the ink decreased. Simultaneously, the fraction of the surface covered by the highly ordered large domains declined, and interstitial regions having molecules in lower density configurations began to appear. This tendency increased until domains of low-density structures filled almost the entire surface, interrupted only by the occurrence of areas without observable order. The distribution of depressions in the uppermost layer of the Au(111) substrate that resulted from the reaction of DDT with gold was also influenced by the ink concentration. STM

revealed long-range spatial correlations between individual recessed regions on the surface at a concentration of 10 mM alkanethiol, whereas the overall density of depressions exhibited a pronounced minimum when SAMs resulted from 1 mM solutions of ink. Together these data provided insight into the method of growth of SAMs on epitaxial films of gold and demonstrated that the processes of μCP provide deterministic and convenient control over this growth.

2. Experimental Section

Chemicals. Dodecanethiol (DDT) (>97%, Fluka) was purified by chromatography (20:1 hexane:ethyl acetate on Silica Gel 60, Fluka). DDT was further refined by freezing its liquid and pumping off the residual gas at ≈1 mTorr. Hexadecane (98%, Fluka) was used without further purification. Ethanol (EtOH) (puriss grade, Fluka) was bubbled for ≈30 s with Ar prior to use. PDMS prepolymer (SYLGARD silicone elastomer 184) and curing agent (SYLGARD silicone elastomer 184 curing agent) were purchased from Dow Corning Corporation. N_2 and Ar had purities >99.999%.
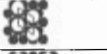
Substrate, Stamp, and SAM Preparation. Epitaxial Au(111) films resulted from resistive evaporation of ≈200 nm of gold (>99.99%, Goodfellow, UK) onto freshly cleaved muscovite mica (Baltec, Liechtenstein) using a BAE-250 evaporation chamber (Balzers, Liechtenstein) at a base pressure of 10^{-7} Torr. The mica substrate was heated to 330 °C prior to, and during, evaporation, and Au was deposited at a rate of 5 Å/s, followed by a 15-min anneal of the film at this temperature. The sample was cooled to below 50 °C prior to its release from vacuum. STM showed that these Au(111) films had atomically flat terraces typically >200 nm in lateral extent. Gold prepared in this way was dewet by a solution of 1 mM dodecanethiol in EtOH within 2 s following its emergence from a 5-s dip in the solution. The elastomeric stamp was formed by pouring a mixture of PDMS prepolymer and its curing agent (10:1 by weight) onto a clean polystyrene Petri dish (Bibby Sterillin, UK). The dish was left at 60 °C for at least 12 h to ensure a complete cure of the polymer mixture. A new stamp, ≈ 6 × 6 mm², was cut from the cured PDMS for each monolayer transfer; printing was done using the side of the stamp that had faced the dish bottom. The stamp was rinsed three times with 10 mL EtOH and dried under a flow of N_2 for 30 s. Two drops (≈0.2 mL) of a freshly prepared (<1 h) solution of DDT in EtOH were placed on top of the rinsed stamp, enough liquid to cover the surface. The liquid remained there for 30 s to allow it to equilibrate with the PDMS surface, after which it was removed quickly (<0.5 s) under a stream of N_2. The flow of N_2 continued for another 30 s after evident disappearance of the bulk drop to evaporate the residual EtOH. Monolayer transfer occurred by placing the stamp on top of a gold substrate under its own weight, where it remained for 10 s unless otherwise noted. The substrate was placed directly in the STM without further rinsing to avoid the effects of solvent on the SAM. For comparison, a monolayer of DDT was prepared by immersion of a Au(111) substrate in a 1-mM DDT/EtOH solution for 18 h. This SAM was rinsed in EtOH after retraction from the adsorption solution.

Contact Angle Measurement. Wettability by water and hexadecane was determined with a Krüss (Hamburg, Germany) contact angle goniometer equipped with a motorized pipette (Matrix Technology, Nashua, NH). A new polypropylene tip was used for each measurement. Three sets of advancing and receding angles, each at a different spot on each sample, were measured on at least three, and in most cases six, different samples at each thiol concentration.

STM Imaging. We used a home-built, low tunneling current STM[14] operating under ambient conditions for imaging. Tips were made by cutting 0.5-mm Pt/Ir (90%/10%) wire (Goodfellow, UK) with surgical scissors. Bias voltages between −0.90 and −0.95 V (tip negative) and tunneling currents from 1 to 10 pA were applied between the tip and sample. Images were acquired in the constant-current mode. The image quality did not depend strongly on the applied bias voltage. We found that nondestructive imaging (i.e., avoidance of scan-induced changes in the appearance of the monolayer) required lower tunneling currents, 1−3 pA, on regions of lower molecular packing densities

(14) Michel, B.; Travaglini, G. *J. Microscopy* **1988**, *152*, 681−685.

Table 1.

Lattice family	Lattice[1]	a	b	γ	Area	Molecules	Density[2]	Packing pattern[3]
$solid_2$	$\sqrt{3} \times \sqrt{3}$	5.0 Å	5.0 Å	120.0°	21.6 Å²	1	100 %	
$solid_2$	$4\sqrt{3} \times 2\sqrt{3}$	10.0 Å	20.0 Å	120.0°	173.2 Å²	8	100 %	
$solid_1$	$3.5 \times \sqrt{3}$	10.1 Å	5.0 Å	84.6°	50.5 Å²	2	86 %	
$solid_1$	$4 \times \sqrt{3}$	11.5 Å	5.0 Å	90.0°	57.5 Å²	2	75 %	
$solid_1$	$8 \times \sqrt{3}$	23.1 Å	5.0 Å	90.0°	115.5 Å²	4	75 %	
$solid_1$	$5 \times \sqrt{3}$	14.4 Å	5.0 Å	90.0°	72.0 Å²	2 (?)	60 %	

[1] Lattices are named by the length of their unit cell vectors relative to the nearest-neighbor spacing of the Au(111) substrate.
[2] The unit cell area divided by the number of molecules per unit cell results in a molecular packing density normalized to that of $solid_2$ domains.
[3] Idealized representations of the packing patterns revealed by STM. The larger white and gray circles represent DDT molecules at different observed heights, whereas the black smaller circles represent the atoms of the uppermost Au(111) layer, which is not normally observed simultaneously in STM measurements. The question marks in the lowermost structure refer to the nondefinitive description of the internal characteristics of the $5 \times \sqrt{3}$ unit cell (see text).

compared to regions of high molecular density. Some of the STM data reduction used the SPIP 96 image processing program.[15]

3. Results and Discussion

In setting out to discover the structure of alkanethiol SAMs formed on gold by μCP, it is worth briefly reviewing what is known more generally about these monolayers. Adsorption of alkanethiols on Au(111) from a solution or the gas phase can result in highly ordered SAMs that cover the entire gold surface. Their thickness measured by ellipsometry suggested a description of the alkyl chains in these monolayers as ordered and extended upright from the surface of the gold.[16] Experiments using reflection-absorption infrared spectroscopy strongly supported this model, demonstrating that the alkyl chains in SAMs were, on average, in an all-trans configuration with a tilt of $\approx$30° from the surface normal.[16,17] Electron,[18] helium,[19] and X-ray diffraction[20] studies of SAMs of alkanethiols on Au-(111) all showed that the adsorbed alkanethiols form a ($\sqrt{3} \times \sqrt{3}$)R30° lattice (see Table 1) commensurate with the underlying gold and anchored, presumably, at 3-fold hollow sites on its surface (but more recent evidence casts some doubt on this conclusion[21]). Poirier and Pylant[22] recently named these ($\sqrt{3} \times \sqrt{3}$)R30° crystalline structures the $solid_2$ phase, a nomenclature also followed here.

Further helium[25] and X-ray[21] diffraction measurements on SAMs subsequently revealed a ($4\sqrt{3} \times 2\sqrt{3}$)$R$30° superstructure (see Table 1) in the monolayer, also calculated in molecular

dynamics simulations.[26] STM studies[27-29] corroborated this finding by displaying the ($4\sqrt{3} \times 2\sqrt{3}$)$R$30° superstructural motif and giving insight into the organization of domain boundaries. In the following discussion we classify these superstructures as subsets of the $solid_2$ family of monolayer phases. The localized visualization of SAMs also showed widely distributed regions in the monolayer depressed by one atomic gold layer. These depressions clearly correlated with the interaction between alkanethiol molecules and the gold surface.[30,31] Conclusions on the cause of their origin are difficult to draw as several mechanisms appear to be operational in parallel, including dissolution of part of the gold surface into the adsorption solution and a reorganization of the uppermost gold layer due to the binding of sulfur.[32]

Figure 1 compares STM images of SAMs formed on gold by μCP to those SAMs formed on gold by its equilibration in solution. A 100-mM solution of DDT in ethanol provided the self-assembling adsorbate for μCP. The appearance of the printed SAM by STM (Figure 1A−C) was indistinguishable from that of a SAM prepared by equilibration of the gold surface in a 1-mM solution for 18 h (Figure 1D−F). Images of SAMs formed by either method of preparation were similar and had common characteristics at all length scales examined (up to 4 × 4 μm²) for several independent sets of comparison. The predominant feature of the images in Figure 1 is the crystalline, ($\sqrt{3} \times \sqrt{3}$)R30° arrangement, of the molecules in the SAMs, some of which appear in one of the three ($4\sqrt{3} \times 2\sqrt{3}$)$R$30° superstructure arrangements observed by STM.[28] No significant difference in the size, type, or distribution of domains existed between the two methods of SAM formation. The dark regions that appear widespread in these sets of images (marked by black arrows in Figure 1C,F) are regions lowered by one Au(111) layer (2.36 Å) by the gold dissolution/reorganization mechanisms mentioned above. When SAMs are made by equilibration in solution, small amounts of gold correlated to the conditions of SAM formation appear in the adsorption bath.[30,31] We do not know where the gold (if any) goes when μCP forms the SAM. Whether the liberated metal remains on top of the monolayer without being imaged by the STM, ends up on, or in, the stamp, or returns to the bulk substrate cannot be resolved at present. Importantly, the processes that give rise to depressions in SAMs formed in solution are still operative in the environment defined by the inked surface of PDMS during μCP. Equally important, molecules fill the depressions using either method of SAM preparation. The arrangement of molecules in the depressed regions is the same as in the surrounding nonrecessed domains. The black arrows in Figure 1C,F point to examples of this similarity in structure. We concluded from the data in Figure 1 that the structure of SAMs formed by μCP or equilibration in solution was not inherently different, despite the dissimilar times of formation and amounts of material available for forming the monolayer in each case. We expected, therefore, similarity in the wettability of SAMs resulting from either process of SAM formation.

(15) Jørgensen, J. F. Danish Institute of Fundamental Metrology, Lyngby, Denmark.
(16) Nuzzo, R. G.; Fusco, F. A.; Allara, D. L. *J. Am. Chem. Soc.* **1987**, *109*, 2358−2368.
(17) Porter, M. D.; Bright, T. B.; Allara, D. L.; Chidsey, C. E. D. *J. Am. Chem. Soc.* **1987**, *109*, 3559−3568.
(18) Strong, L.; Whitesides, G. M. *Langmuir* **1988**, *4*, 546−558.
(19) Chidsey, C. E. D.; Liu, G.; Rowntree, P.; Scoles, G. *J. Chem. Phys.* **1989**, *91*, 4421−4423.
(20) Fenter, P.; Eisenberger, P.; Liang, K. S. *Phys. Rev. Lett.* **1993**, *70*, 2447−2450.
(21) Fenter, P.; Eberhardt, A.; Eisenberger, P. *Science* **1994**, *266*, 1216−1218.
(22) Poirier, G. E.; Pylant, E. D. *Science* **1996**, *272*, 1145−1148.
(23) Häussling, L.; Michel, B.; Ringsdorf, H.; Rohrer, H. *Angew. Chem., Int. Ed. Engl.* **1991**, *30*, 569−572.
(24) Alves, C. A.; Smith, E. L.; Porter, M. D. *J. Am. Chem. Soc.* **1992**, *114*, 1222−1227.
(25) Camillone III, N.; Chidsey, C. E. D.; Liu, G.; Scoles, G. *J. Chem. Phys.* **1993**, *98*, 3503−3511.

(26) May, W.; Klein, M. L. *Langmuir* **1994**, *10*, 188.
(27) Poirier, G. E.; Tarlov, M. J. *Langmuir* **1994**, *10*, 2853−2856.
(28) Delamarche, E.; Michel, B.; Gerber, Ch.; Anselmetti, D.; Güntherodt, H.-J.; Wolf, H.; Ringsdorf, H. *Langmuir* **1994**, *10*, 2869−2871.
(29) Schönenberger, C.; Jorritsma, J.; Sondag-Huethorst, J. A. M.; Fokkink, L. G. J. *J. Phys. Chem.* **1995**, *99*, 3259−3271.
(30) Schönenberger, C.; Sondag-Huethorst, J. A. M.; Jorritsma, J.; Fokkink, L. G. J. *Langmuir* **1994**, *10*, 611−614.
(31) Sondag-Huethorst, J. A. M.; Schönenberger, C.; Fokkink, L. G. J. *J. Phys. Chem.* **1994**, *98*, 6826−6834.
(32) McDermott, C. A.; McDermott, M. T.; Green, J.-C.; Porter, M. D. *J. Phys. Chem.* **1995**, *99*, 13257−13267.
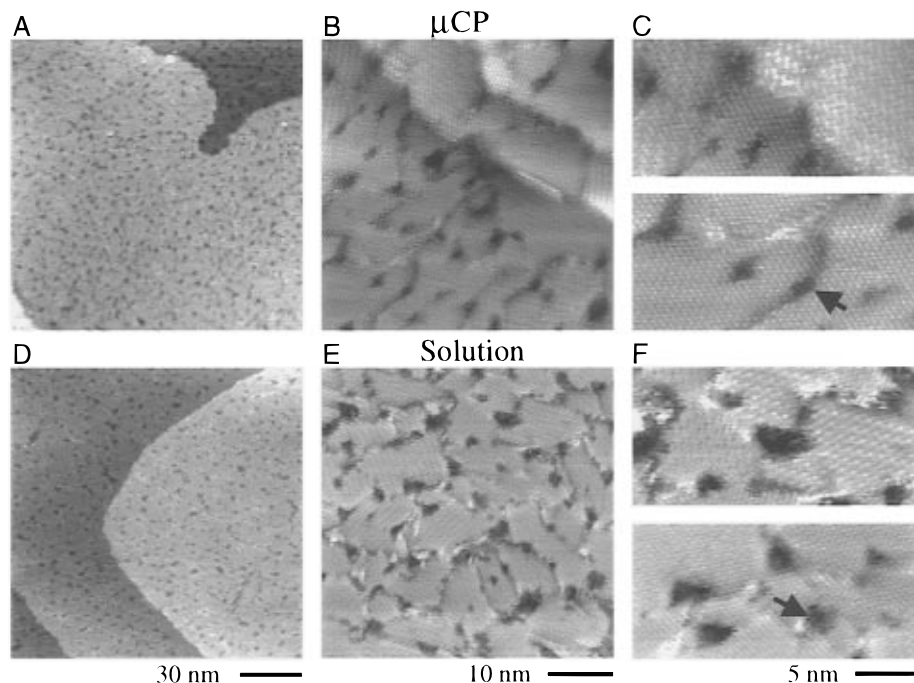
Figure 1. Comparison of STM images of SAMs printed on Au(111) by μCP using a 100-mM DDT ink (**A**, **B**, **C**) and SAMs formed by equilibration of Au(111) in a 1-mM solution of DDT in ethanol for 18 h (**D**, **E**, **F**) shows their similarity. The arrows in **C** and **F** point to depressed areas in the monolayers that display structural motifs similar to that of the surrounding, elevated, regions in the SAM (see text). The gray scale reflects a height difference of 4 Å.

Bain and co-workers used, with striking success, the wettability of surfaces to infer microscopic phenomena by correlating the structures of SAMs with this macroscopic measure.[33,34] Contact angles of water and hexadecane on SAMs formed by μCP or equilibration in solution indeed confirmed our expectation of their indistinguishable wetting behavior, Figure 2. We decided to extend this study of the wettability of printed SAMs to probe the apparent effects of varying the thiol concentration in the solution used to ink the stamp. No SAM forms in the absence of DDT on the stamp, of course, so progressively lower concentrations in the ink should, at some point, result in less complete SAMs. We used the same procedure to ink the stamp, each time equilibrating its surface with a solution of DDT for 30 s prior to removal of the liquid under a stream of nitrogen. Some type of SAM formed by printing with stamps inked using solutions of DDT ranging over six orders of magnitude in concentration (from 1 μM to 1 M). Here, and in the subsequent sections, we used a duration of 10 s for contact between the stamp and the surface, although we did not notice a great sensitivity to this time: Contact angles and STM images of SAMs formed during 1−30 s of contact between stamp and gold could not be distinguished (see below). Figure 2 shows the change in wettability of SAMs formed by μCP with stamps inked by different concentrations of DDT. The trend toward higher wettability and greater hysteresis between the advancing and receding contact angles is evident in the figure at inking concentrations below $\approx$10 mM. Measurements on gold exposed to the laboratory environment or printed by a stamp inked with $\leq$10 μM DDT were indistinguishable and provided the limit of useful observation of the wettability of the system (data not shown). When we followed the method of inking the stamp surface outlined above, the contact angles and their hysteresis were reproducible even at very low ($\leq$1 mM) concentrations of DDT so that the printing process remained deterministic.
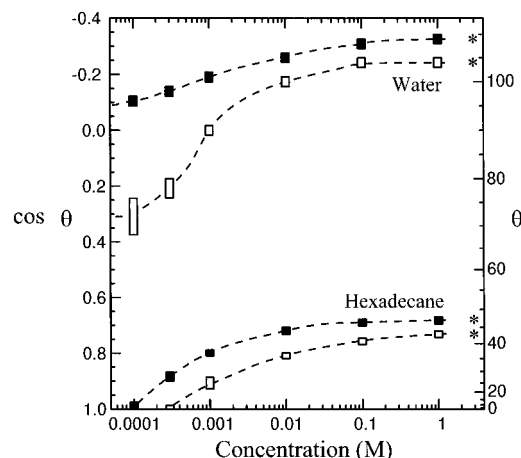

Figure 2. The wettability of printed SAMs depended on the concentration of DDT used to ink the stamp. The range in measurement of the advancing (solid symbols) and receding (hollow symbols) contact angles is given by the size of the symbol. Limiting values for these angles found on SAMs equilibrated in 1-mM solutions of DDT for 24 h are denoted by the stars shown at the right-hand side of the graph. The dashed lines are provided as guides to the eye.

The observed reproducibility of macroscopic characteristics of these monolayers was similarly paralleled in the molecular-scale structure of the printed SAMs (see below). The changes in wettability of the printed SAMs strongly suggested corresponding transformations in their microscopic organization. Previous studies showed that contact angles on a SAM reflect its composition and degree of completion[33,35,36] although a molecular-scale description of the origin of these changes remained elusive in many details. A variety of SAMs exhibiting arrangements of low molecular density are known, or inferred, for monolayers prepared from the gas of a thiol under vacuum

(33) Bain, C. D.; Troughton, E. B.; Tao, Y.-T.; Evall, J.; Whitesides, G. M.; Nuzzo, R. G. *J. Am. Chem. Soc.* **1989**, *111*, 321−335.

(34) Bain, C. D.; Whitesides, G. M. *Science* **1988**, *240*, 62−63.

(35) Tidswell, I. M.; Rabedeau, T. A.; Pershan, P. S.; Kosowsky, S. D.; Folkers, J. P.; Whitesides, G. M. *J. Chem. Phys.* **1991**, *95*, 2854−2861.

(36) Tidswell, I. M.; Rabedeau, T. A.; Pershan, P. S.; Kosowsky, S. D.; Folkers, J. P.; Whitesides, G. M. *J. Chem. Phys.* **1993**, *98*, 1754.
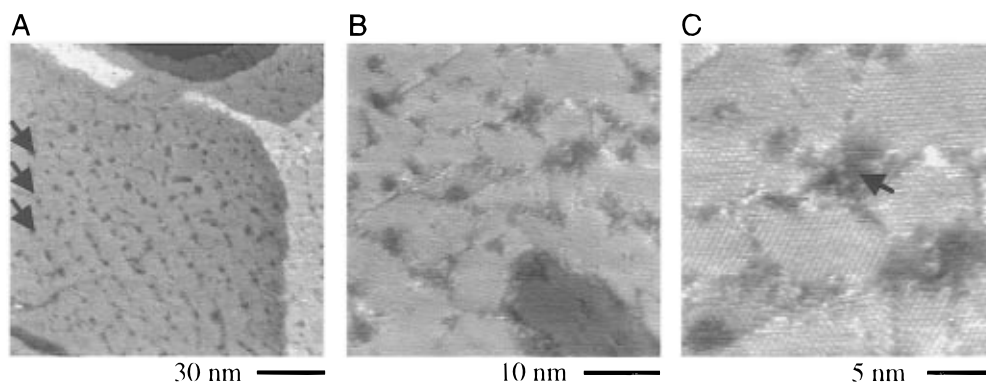
Figure 3. STM images of SAMs printed using 10-mM solutions of DDT in ethanol showed a tendency toward the organization of depressions in the gold surface. The arrows in **A** point to columns of depressions in the SAM, in some cases extending across entire terraces on the gold surface. These depressed regions typically had a SAM with a packing pattern that corresponded to that of the surrounding, elevated SAM (arrow in **C**).

conditions, including the organization of molecules in expanded lattices and even more disordered 2D gas structures.[37-40] SAMs prepared by brief adsorption in micromolar solutions of thiol exhibited similarly structured arrangements.[22,29] How these structures correlated to SAMs formed by μCP, if at all, remained open. It appeared from our wettability measurements that μCP was capable of precise, and convenient, formation of monolayers having intermediate densities, so we decided to pursue their characterization by STM. We were particularly interested in understanding more fully what other types of organization in SAMs formed by μCP were possible and perhaps exploitable, and in understanding the microscopic origins of the changes in wetting in these SAMs.

Reducing the thiol concentration to 10 mM in the solution used to ink the stamp led to the formation of SAMs by μCP that appeared complete when imaged by STM, Figure 3. Once again the surface of the gold was evidently covered by crystalline domains of trans-extended alkanethiols organized in the characteristic $(\sqrt{3} \times \sqrt{3})R30°$ structure with some domains displaying $(4\sqrt{3} \times 2\sqrt{3})R30°$ superstructures. The size of domains tended to be larger, at the 10-nm level here, than SAMs printed with inks at higher concentrations (>10 mM). Further, a striking difference between these two cases appeared in the organization of depressions in SAMs printed at the lower concentration: The depressions arranged themselves into columns along one of the three symmetry axes characteristic of the underlying Au(111) substrate. The columns were separated by 10.4 ± 0.3 nm parallel to one of the $solid_2$ crystallite's nearest-neighbor directions and extended over hundreds of nanometers (see Figure 3A). Arrays of molecules exhibiting the $(\sqrt{3} \times \sqrt{3})R30°$ structure appeared in most depressed areas, suggesting that molecules also fill up the majority of the depressions at this ink concentration (black arrow, Figure 1C). Boundaries of $solid_2$ domains in the SAM showed the same tendency as the depressions to align along dominant lattice directions of the gold substrate, an observation not readily apparent for SAMs printed at higher concentrations (cf. Figure 1). The origin of the spatial correlation between depressed regions is unclear at present. We speculate that one cause could be a higher probability for nucleation of depressions at elbow sites of the compressed gold herringbone structure at this thiol concentration during the initial steps of growth.[22] This reflects,

(37) Poirier, G. E.; Tarlov, M. J.; Rushmeier, H. E. *Langmuir* **1994**, *10*, 3383−3386.
(38) Camillone III, N.; Eisenberger, P.; Leung, T. Y. B.; Schwartz, P.; Scoles, G.; Poirier, G. E.; Tarlov, M. J. *J. Chem. Phys.* **1994**, *101*, 11031−11036.
(39) Poirier, G. E.; Pylant, E. D.; White, J. M. *J. Chem. Phys.* **1996**, *105*, 2089−2092.
(40) Kang, J.; Rowntree, P. A. *Langmuir* **1996**, *12*, 2813−2819.
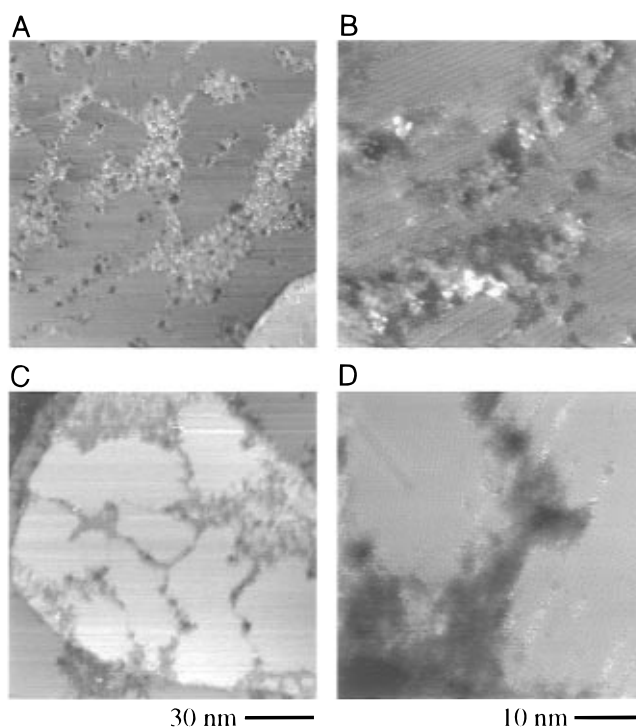
Figure 4. The appearance of SAMs printed using 4-mM solutions of DDT in ethanol was largely unaffected by the duration of contact between the stamp and the Au(111) surface for times <30 s. The STM images reveal the organization of printed SAMs resulting from 0.3 s (**A** and **B**) and 3 s (**C** and **D**) of contact between the substrate and inked PDMS. Longer durations of contact (up to 30 s, data not shown) showed a similar insensitivity of monolayer organization to this aspect of μCP.

perhaps, a relationship between growth of domains of SAMs and structural rearrangements of the gold substrate.

Inks containing 10-mM DDT were the lower limit for the formation of complete SAMs. Below this concentration very significant changes in the appearance of the monolayers were observed. Ink concentrations of 4 mM caused the average size of $solid_2$ domains in printed SAMs to increase to $\approx 30-50$ nm, whereas individual domains became separated by narrow regions of lower height having no apparent order, Figure 4. The duration of contact between the stamp and the gold surface could not be obviously correlated to domain sizes or separations. Figure 4A,B show STM images of SAMs formed during a contact time of ≈ 0.3 s, whereas a longer contact of ≈ 3 s resulted in the structures displayed in Figure 4C,D. Our observations emphasize a special role of PDMS in μCP: PDMS evidently allows rapid diffusion of DDT into its bulk. The PDMS
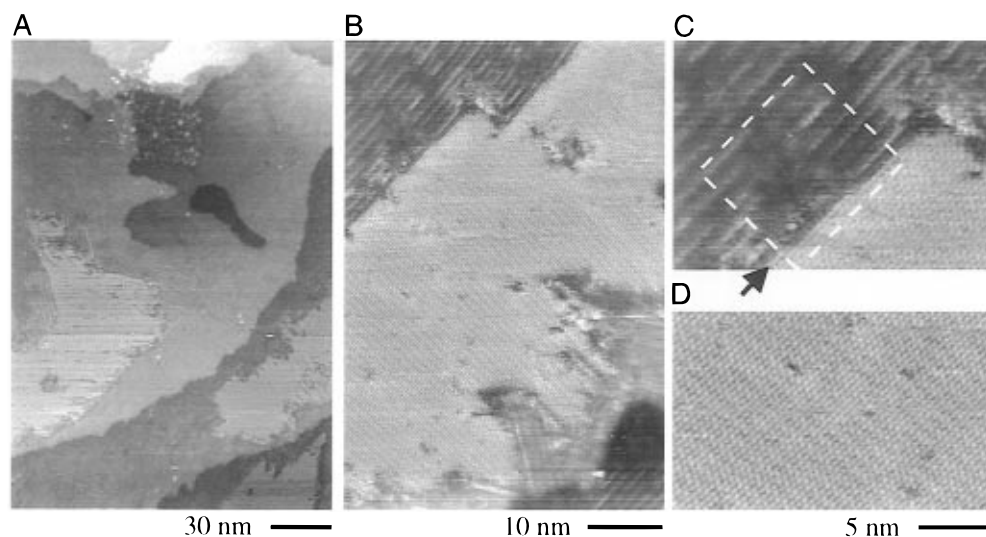
Figure 5. SAMs printed using 1-mM concentrations of DDT had large (often >50 nm on a side) crystallites of the *solid₂* phase and displayed a distinct minimum in the number of depressions evident on the gold surface. A second, lower density phase (*solid₁*) of characteristic monolayer organization appeared in the STM images highly correlated to the first higher density phase. The arrow in **C** marks the end of a column of adsorbed DDT in the *solid₂* phase and its continuance in a *solid₁*-type packing. The rectangular region shows the area of enlargement in Figure 6.

polymer matrix can incorporate significant amounts of adsorbate (alkanethiol) molecules as proven by its ability to form μCP monolayers even after thorough drying of its surface by a flow of nitrogen. The amount of incorporated adsorbate material, presumably in the gas phase, and its penetration depth into the bulk of the stamp is not obvious from our measurements. The observation of a sensitivity of printed SAMs to the inking concentration and a significant *insensitivity* to the duration of printing suggest, however, that adsorbate vapor-phase equilibration takes place throughout extensive parts of the stamp during the inking process and that subsequent release of adsorbate molecules to the surface region during the printing process is limited by vapor-phase diffusion. This description of the adsorbate distribution within the polymer matrix is supported by the observation that a stamp inked once may form a number of monolayers exhibiting similar degrees of completion and order. The result suggests that the degree of completion of the SAM is not simply limited by depletion of thiol from the surface of the stamp during printing. Instead, the gold surface arrives very quickly (<0.3 s) to a limiting state where further adsorption is inhibited by the existing monolayer, demonstrating in this system how the final state of the SAM is largely governed by the initial flux of molecules to the gold surface.

The tendency toward larger isolated *solid₂* crystalline domains in printed SAMs became stronger upon reduction of the concentration of the stamping solution to 1 mM. Here, the average size of a domain increased to 50−200 nm (Figure 5A,B), one order of magnitude larger than observed after any other preparation method at room temperature. Structurally, these highly ordered regions displayed a $(\sqrt{3} \times \sqrt{3})R30°$ lattice with a $(4\sqrt{3} \times 2\sqrt{3})R30°$ superlattice structure (Figure 5D). All *solid₂* crystallites investigated exhibited the same superstructural motif, namely the δ packing pattern ("zigzag" packing, cf. Table 1) described by Delamarche et al.[28] Whether this observation is inherent to SAMs printed with 1 mM inking solutions or is the consequence of insufficient observation remains open.

The large crystallites of the *solid₂* family of phases covered 20−40% of the surface with an average distance between crystallites of up to hundreds of nanometers. Regions between *solid₂* crystallites were almost completely covered by a striped phase with characteristics resembling the $p \times \sqrt{3}$ packing

pattern previously observed by helium diffraction[38,41] and STM.[37,38] Poirier and Pylant named this family of phases *solid₁*[22] (see Table 1). Detection of *solid₁* domains by STM occurred with somewhat lower resolution than regions having *solid₂* domains, although we think the images reflected the presence of real structures in the monolayer: Our observations were consistent for different samples prepared similarly and imaged by different tips under different tunneling conditions and in a variety of scanning directions. We often observed these families of expanded, striped phases adjacent to structures in the same image having the characteristic c (4 × 2) organization of *solid₂* domains.

STM images of the striped phases resolved some aspects of the molecular organization of the individual bright stripes. Each stripe apparently consists of a single line of molecules with a spacing between molecules of 5.0 ± 0.1 Å. Here, and below, we used the well-known structural parameters of the *solid₂* domains, imaged within the same frame, as internal calibration parameters. The stripes in the *solid₁* domains were aligned along the next-nearest-neighbor directions of the Au(111) substrate (deduced by comparison with the known orientational correlation between the gold and the $(\sqrt{3} \times \sqrt{3})R30°$ lattice) with average domain sizes of ≈30 Å and often elongated in the direction of the stripes. We observed that the spacing between parallel bright stripes of molecules varied considerably. Fourier analysis of the regions covered by the *solid₁* family of phases revealed a prevailing spacing of 14.4 ± 0.2 Å corresponding to a rectangular 5 × $\sqrt{3}$ lattice (14.4 × 5.0 Å²) within the experimental uncertainty (cf. Table 1). This structure was characteristic of the molecular organization at distances of more than 10 nm from the edges of *solid₂* crystallites. Closer to these higher density domains, STM images displayed a range of monotonously decreasing spacings of the striped phases, in effect a transition zone (Figure 5C) between the lattice spacings of the hexagonal *solid₂* phase and that of the prevailing rectangular 5 × $\sqrt{3}$ *solid₁* structure.

The gradual transition from lower to higher density arrangements of the molecules can be described in terms of the STM image as a stepwise compression of bright lines of the striped phases, ending as next-nearest rows of molecules in the

(41) Camillone III, N.; Leung, T. Y. B.; Schwartz, P.; Eisenberger, P.; Scoles, G. *Langmuir* **1996**, *12*, 2737−2746.
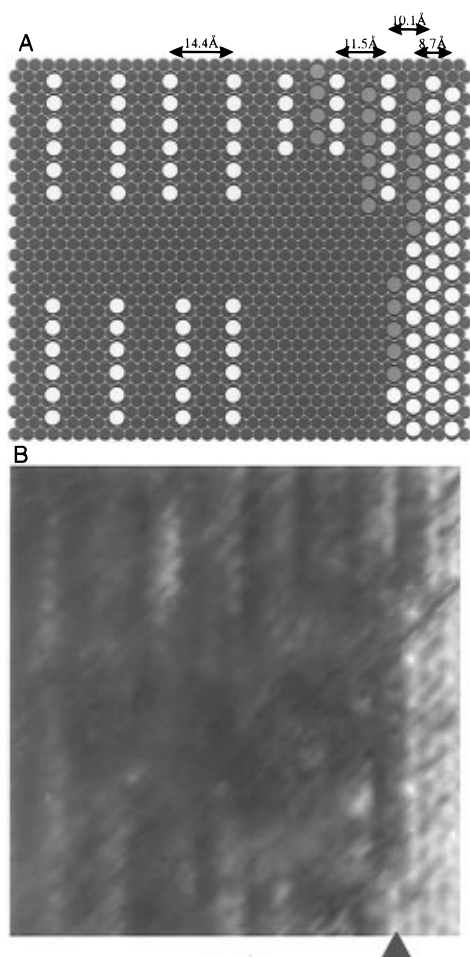
Figure 6. The transition region in domains of *solid*$_2$ (right) to *solid*$_1$ (left) phases is imaged by STM. The imaged region (**B**), a zoom of the area marked in Figure 5, is shown below a scheme (**A**) representing the hypothesized exact positions of the adsorbed DDT (white and gray circles reflecting molecules of different heights) on the gold substrate (black circles). The spacings indicated reflect expected values for a Au(111) lattice and are not experimental data (see text).

hexagonal lattice of a *solid*$_2$ crystallite. This transition is most easily visualized through the opposite process, i.e., the expansion of the crystallite phase to the striped phase. For clarity, Figure 6B presents a zoom of the transition region indicated by a rectangle in Figure 5C. Figure 6A displays a corresponding drawing of the positions of individual molecules (white and gray circles) situated on top of the Au(111) lattice (black circles). Following the line of molecules at the crystallite boundary indicated by the black arrow in Figure 6B (and in Figure 5C), the apparent height of the molecules suddenly decreases by ≈ 1 Å (from white to gray bumps in the STM image), but individual molecules remain resolved (gray circles). Approximately the next dozen molecules exist in a recessed state until the next row of molecules exposed at the crystallite boundary fades to the lowered state. At this point the molecules in the marked line recur at almost the same height as the *solid*$_2$ crystallite but laterally displaced by a distance of 1.4 ± 0.2 Å perpendicular to the crystallite edge. This corresponds to an increase of the distance between next-nearest rows of molecules by half the nearest-neighbor spacing of the underlying Au(111) substrate (*cf.* Figure 6A). The new monolayer structure can be described as a $3.5 \times \sqrt{3}$ (10.1×5.0 Å^2), almost rectangular, superlattice (cf. Table 1). The intervening line of recessed molecules is difficult to resolve at the molecular level, but the line retains its lateral spacing to the crystallite edge, implying that there is
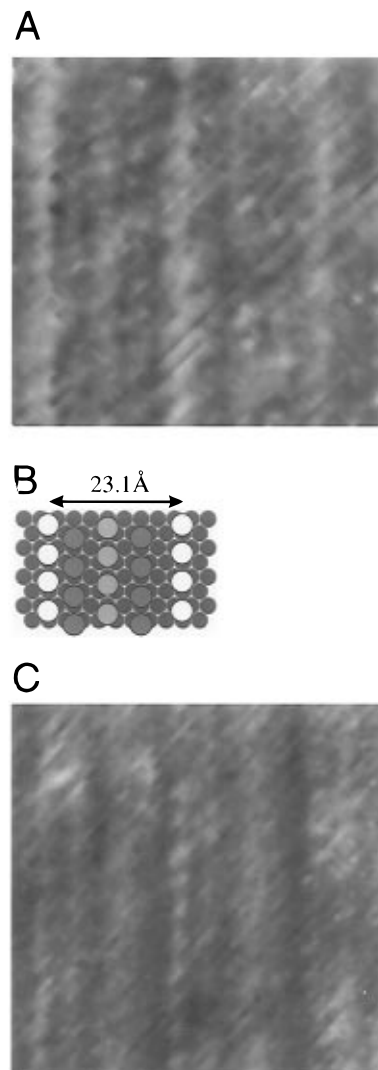

Figure 7. STM imaging of some low-density phases in printed SAMs showed a sensitivity to repeated scanning during acquisition of successive images (**A** and **C**). The scheme in **B**, represented as in Figure 6, indicates the positions for DDT adsorbed in a $8 \times \sqrt{3}$ lattice on Au(111) with relative heights corresponding to image **A**.

a geometrical relation between the molecules at the edge of the *solid*$_2$ phase and the line of lowered molecules. This observation suggests that the anchoring points of the individual molecules to the Au(111) substrate remain the same and that the apparent lowering is due either to an increase in the available space created by the displacement of the next line of molecules or to a lowering of the tunneling probability, possibly induced by a decrease in the chain order parameter.[42] Beyond the recurred line of molecules only the bright lines in the striped structures are resolvable at the molecular level, but computation of the average height perpendicular to the bright lines allows determination of the exact positions of the constituent unresolved molecules. Measurements show a bright line-to bright line spacing of 11.6 ± 0.2 Å for the next three lines, corresponding to an increase of the crystallite next-nearest row spacing by 2.9 ± 0.2 Å or, within the uncertainty, one nearest-neighbor distance of the Au(111) lattice. These parameters agree with a $4 \times \sqrt{3}$ (11.5×5.0 Å^2) rectangular overlattice. Looking farther away from the crystallite edge, we observe what appears to be the limiting case for this system, corresponding to a bright line to bright line spacing of 14.5 ± 0.2 Å, an expansion of the

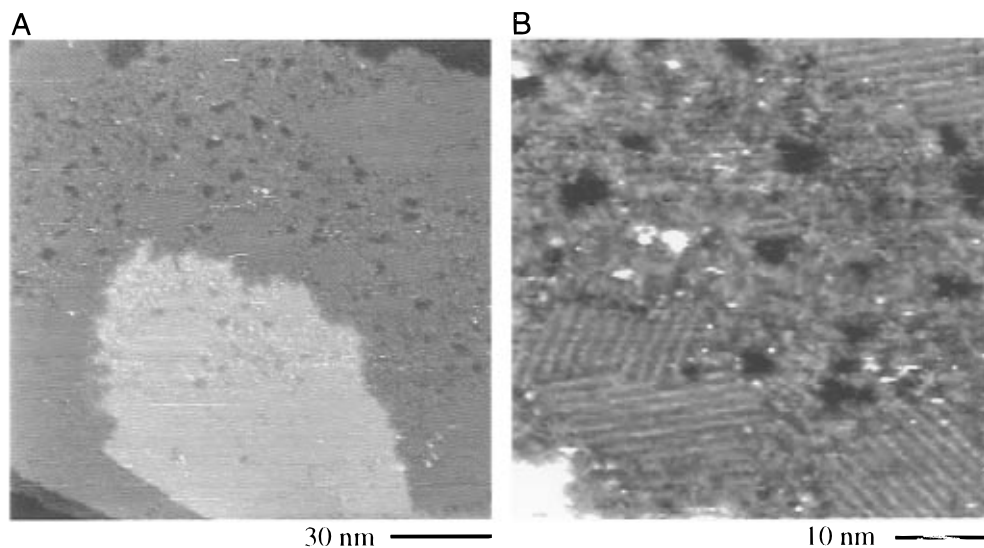(42) Haran, A.; Waldeck, D. H.; Naaman, R.; Moons, E.; Cahen, D. *Science* **1994**, *263*, 948−950.

A   B

30 nm ━━━━━   10 nm ━━━━

Figure 8. SAMs printed using DDT at concentrations of 100 μM showed regions of the *solid*$_1$ phase surrounded by areas having no order discernible by STM. The latter were particularly sensitive to the apparent effects of contaminants, imaged by the STM as irregular bright spots. The large region in **A** that appears white is a gold terrace largely covered by *solid*$_1$ domains.

crystallite next-nearest row spacing by 5.8 ± 0.5 Å or twice the Au(111) nearest-neighbor distance, giving the $5 \times \sqrt{3}$ (14.4×5.0 Å^2) lattice observed over most parts of the surface. Beyond this spacing, i.e., at lattice spacings larger than 14.4 Å (approximately the length of a molecule of DDT), the molecules in SAMs of DDT apparently no longer have sufficient intermolecular interactions to maintain a static regular structure discernible by STM.

Another member of the *solid*$_1$ family of phases occupied parts of the surface close to *solid*$_2$ crystallites. This phase can be described as a doubled $4 \times \sqrt{3}$ structure in which every second bright line is shifted perpendicular to the direction of the bright line by half a nearest-neighbor spacing of the underlying gold lattice, giving an $8 \times \sqrt{3}$ (23.1×5.0 Å^2) rectangular unit cell (cf. Table 1). The STM occasionally imaged the structure in a manner similar to the double "pinrows" of molecules reported previously.[22,37] Repeated scanning of the same area, however, displayed the double $4 \times \sqrt{3}$ type of structure. Figure 7 shows an example of the varying appearance of the $8 \times \sqrt{3}$ lattice with a horizontally aligned scheme of the molecular positions. Both images were recorded over exactly the same region of the SAM with ten intervening scans between the two recordings. This observation emphasizes that STM investigations of exact molecular organization patterns under ambient conditions can be ambiguous due to local variations in the probe properties *and* to the surroundings that may prevail at an atomic scale during data acquisition. Our measurements do not permit a definitive distinction between the double or single pinrows as being the most accurate description of this particular phase. We think, however, that the consistent appearance of the other members of *solid*$_1$ phase family as single pinrows supports the latter description of the $8 \times \sqrt{3}$ lattice. Equivalent $8 \times \sqrt{3}$ structures have been observed in our laboratory on SAMs adsorbed from ethanolic thiol solutions and subsequently exposed to a short thermal anneal that causes a loss of molecules from the SAM and an overall decrease in its density. Thus, this packing motif seems to be thermodynamically favored over the simple $4 \times \sqrt{3}$ pattern at equivalent molecular packing densities (cf. Table 1).

A unifying component of the structural parameters of the phases observed in SAMs formed by μCP of 1-mM thiol solutions is the strong templating effect of the underlying gold

substrate. The short lattice vector (5.0 Å) of all the phases is given by the shortest distance between equivalent 3-fold hollow sites in the uppermost Au(111) layer that do not share any of their anchoring gold atoms. Perpendicular to the common short lattice vector, the *solid*$_1$ (and the $(4\sqrt{3} \times 2\sqrt{3})R30°$ *solid*$_2$ superstructure) phases have long lattice vectors that are integer multiples of the spacing between nearest neighbors in the Au-(111) surface layer. The $3.5 \times \sqrt{3}$ structure constitutes a minor exception to this pattern, but its transitory nature would also suggest that it is a lattice of less stability than the other *solid*$_1$ phases observed.

Small depressed regions were scattered over the surface at a relatively low density compared to SAMs formed from both higher or lower (see below) DDT concentration inks. The lateral distribution of depressions and the sizes and shapes of *solid*$_1$ and *solid*$_2$ domains seemed to be highly correlated, suggesting depressions acted as pinning sites for monolayer organization, at least above a certain size, that could not be circumvented by growing domains. This correlation had previously been observed by slow, vapor-phase dosing of mercaptohexanol under vacuum conditions, clearly showing that the formation of organized phases of thiols was spatially correlated to the creation of depressions.[22] Here, the depressions remained fixed at room temperature, once formed, and pinned the growth of ordered domains at the depressed sites. It is not clear why we observe the very low density of depressions under these specific preparation conditions, though this observation was highly reproducible for SAMs formed by μCP at 1−4 mM DDT concentrations. The discovery of such controllable and convenient growth conditions for SAMs of alkanethiols on Au suggests strategies to augment the level of achievable order in monolayers on epitaxially grown substrates.

Microcontact printing with solutions containing 100 μM led to the disappearance of *solid*$_2$ domains. STM imaged a surface almost completely covered by *solid*$_1$ domains with intervening regions without observable signs of order but with a relatively large density of depressions, Figure 8A (please note that the large bright region in Figure 8A results from a gold terrace). Schönenberger et al.[29] previously observed similar regions without order and ascribed them to a 2D liquid-like state. STM measurements were rather difficult to perform on these parts of the printed SAM because of intermittent current spikes during

normal scanning of the sample and evident as saturated white spots in the topological images. We observed this phenomenon principally on regions having no detectable SAM (in either *solid*$_1$ or *solid*$_2$ types of organization), correlated to areas of relatively high surface energy in the SAM, reflected by the relatively greater wettability of these printed monolayers. We think the current spikes correspond to the presence of adsorbed contaminants on the film that somehow "short" the tunneling junction, perhaps electrochemically or capacitively. In any case, these results emphasize how effectively the presence of an organized, hydrophobic SAM controls the electronic properties of the gold interface.

The lattice parameters of the *solid*$_1$ domains formed at 100 μm thiol concentration were determined with less accuracy compared to the 1-mM sample due to the lack of an internal calibration standard (i.e., the *solid*$_2$ domains). We measured bright line spacings of 14.2 ± 0.4 Å (using the instrument calibration) compatible with a $5 \times \sqrt{3}$ overlattice within the experimental uncertainty. Table 1 summarizes all of our STM observations of the molecular phases in printed SAMs of DDT on gold. The second molecules of a two-molecule unit cell of the $5 \times \sqrt{3}$ structure has not been resolved unambiguously, but its existence seems highly probable based on the pattern of slowly decreasing molecular density formed by the other resolved structures.

Depressions within the orderless surface regions (Figure 6B, black arrow) were ≈2.4 Å lower than the surrounding parts of the surface. The close resemblance to the thickness of one Au-(111) layer (2.36 Å) suggests that the degree of coverage in the recessed patches and in the orderless state is the same, as a significantly lower density of molecules presumably would result in an even larger height difference as measured by STM. The observation of depressions in the midst of apparently orderless regions provided further evidence that the processes giving rise to depressed regions were not strictly correlated to the formation of ordered domains, i.e., both processes are uncoupled consequences of reactions between thiols and gold whose products interact at increasingly high coverage of the gold substrate. This interpretation is in agreement with the results of Poirier and Pylant,[22] who observed *nucleation* of ordered domains and depressed regions without obvious spatial correlation.

4. Conclusion

The discovery of the molecular structure of SAMs formed by μCP and the observation that, under some experimental conditions, these monolayers are indistinguishable from those formed in solution is important for several reasons. First, it helps us understand why printed SAMs have potential in technology: They can provide a surface coverage high enough to leave it free of defects, reaching a density of thiol on gold that causes them to order and crystallize. Second the Au(111) surface is not obviously disturbed by the printing step, suggesting that the stresses associated with this method of application of thiol are negligible for the gold-/-DDT-/-PDMS system. Gold is soft, and its surface atoms are mobile at room temperature. Microcontact printing with PDMS did not cause exceptional disruption of the basic epitaxial organization of the gold surface, however, as terraces and steps remained largely evident on the substrate except where the processes associated with a chemical reaction of DDT with gold mediated its structure. Third, despite the lack of rinsing, the monolayers appeared free of residues from the printing process such as excess thiol, contaminants already on the gold surface, residues extracted from the PDMS, or gold clusters liberated by the reaction with DDT. This result suggests the power of the covalent self-assembly schemes and their ability to define and control macroscopic interfaces by nanometer-scale assembly that we infer removes and keeps away otherwise confounding materials in a way not possible with other organizational techniques like Langmuir−Blodgett film formation. Fourth, μCP SAMs provide a wonderful opportunity to observe and control the emergence of order in monolayer films at the nanometer scale and its effects on microscopic and macroscopic properties of these films.

The formation of printed SAMs shares many attributes with their formation through the vapor phase.[22] When very small concentrations of DDT ($<$100 μM) are used as an ink, printed molecules stick randomly to the gold surface forming a disordered (perhaps liquid-like) state. With sufficiently high local molecular density ($<$60% of the maximum coverage observed in *solid*$_2$ crystallites), regions of the surface recessed by one atomic gold layer nucleate. Still higher local concentrations of thiols ($>$60% of maximum coverage) result in the nucleation and growth of semiordered *solid*$_1$ type islands exhibiting a $5 \times \sqrt{3}$ packing motif from the disordered state. Microcontact printed SAMs reach this point at ink concentrations of thiol close to 100 μM, and, above this concentration, the area fraction of these *solid*$_1$ domains increases toward unity, covering the entire surface at ink concentrations between 100 μM and 1 mM. Increasing the concentration of surface-bound thiols results in a compression of the two-molecule unit cell to incorporate the surface excess and leads to the observation of two-molecule $4 \times \sqrt{3}$ and four-molecule $8 \times \sqrt{3}$ structures having packing densities of 75% of maximum coverage. A further increase in the local molecular density gives rise to a transitory $3.5 \times \sqrt{3}$ structure ending in the nucleation and growth of dense *solid*$_2$ domains. We expect that future molecular dynamics simulations of the adsorption process would prove highly useful in illuminating the details of this transition process.

Ink concentrations close to 1 mM cause the nucleation of the *solid*$_2$ domains (i.e., regions of maximum coverage) to remain a relatively rare event in printed SAMs, thus allowing individual domains to grow to remarkably large sizes that approach the dimensions of single gold terraces. The formation of large *solid*$_2$ domains is concomitant with an observed minimum in the density of gold depressions that would otherwise pin these crystalline domains. It is not obvious why the depressions act as pinning sites for the growth of *solid*$_1$ and *solid*$_2$ domains. We have so far never observed a single crystallite completely incorporating a recessed region. Close analysis of images that appear to show enclosed depressions has always revealed that the enclosure arose by coalescence of two or more individual domains pinned on either side of the depressed area.

Increasing the thiol concentrations from 1 toward 10 mM results in higher total coverage of the gold by *solid*$_2$ crystallites at the expense of the *solid*$_1$ domains. The larger density of thiols evidently also gives rise to higher nucleation rates of *solid*$_2$ domains *and* more depressions, overall yielding a surface covered by more, and smaller, crystallites. A virtual snapshot of the transition in SAMs from growth conditions that give large, single domains to one of small, multiple domains is provided by printed SAMs formed with 4-mM inks of DDT. The transition process is effectively complete at an ink concentration of 10 mM, where almost all of the surface is covered by small (≈10-nm-wide) high-density *solid*$_2$ crystallites separated at corner points by depressed regions. Above this concentration, the structures of printed SAMs are indistinguishable from those formed by adsorption in solution.

The close correspondence between the growth of SAMs by vapor-phase deposition and by μCP, as described above, is not surprising. Macroscopic experiments on the vapor-phase transport of DDT from the surface of a stamp inked by our procedure demonstrate the formation of SAMs when the stamp surface is held within 1 mm of the gold surface. This indicates that the vapor pressure of DDT above the stamp surface can be substantial, perhaps even more so in the microenvironment formed by a PDMS stamp in contact with a gold surface. It is nonetheless fascinating that μCP is capable of forming a high-density monolayer within a fraction of a second. The apparent insensitivity of this process of SAM formation to the duration of contact with the stamp (for times >0.5 s) reinforces the peculiar role of the PDMS in controlling both the magnitude and time scale of mass transport to the surface. The ability to find concentrations of ink that give rise to well-defined, reproducible conditions of growth of printed SAMs can surely aid future experiments that seek to explain, or exploit, the various properties of monolayers formed by this technique.

JA964090C